Sliding Mode Control of a Switched Reluctance Motor Drive with Four-Switch Bi-Directional DC-DC Converter for Torque Ripple Minimization

Ertugrul Ates
ertugrul.ates@agu.edu.tr

Burak Tekgun
burak.tekgun@agu.edu.tr

Gunyaz Ablay
gunyaz.ablay@agu.edu.tr

Dept. of Electrical-Electronics Engineering
Abdullah Gul University
Kayseri, Turkey

***Abstract*— In this paper, a method to drive switched reluctance motors (SRM) with a modular four-switch bi-directional DC-DC converter and an H-bridge is proposed. The DC-DC converter operates as a buck or a boost converter with constant frequency to control each phase current while the H-bridge inverter switches only twice in a period to adjust the polarity of the phase voltage. Sliding mode control is designed to have fast and robust current control in the DC-DC converter. The sliding surface equation which is derived for all operation modes including buck and boost modes in motoring and regenerating conditions is defined with the estimated inductor current. The proposed drive system eliminates the bulk DC-capacitors and allows one to adjust the bus voltage individually for all phases. Moreover, the proposed system topology works with only one high-frequency switching device in the DC-DC conversion stage rather than two in conventional drives which provides a simpler current control and reduced switching losses.**

Keywords*— *Switched reluctance motor, sliding mode controller, bi-directional DC-DC converter.

I. INTRODUCTION

Switched reluctance motor (SRM) drive systems have become an attractive candidate for replacing many applications owing to its simple structure, low-price, fault-tolerant features. However, SRMs have some disadvantages such as high torque ripple and acoustic noise in comparison to AC machines. Regardless of their complex control structures, the developments in modern power electronics and digital control systems allow using switched reluctance machines in variable speed applications and increase their popularity [1]–[4].

Typically, the SRM drive includes a power converter that supplies electrical energy to the SRM, a controller, and a rotor position sensor that feeds the rotor position information back to the controller. The power converter is used to excite each phase of the SRM and it has specific control structures to control the switching states. The electrical energy is supplied from the power converter to the SRM, it generates the required positive and negative voltages to increase and decrease the flux in the phase windings [5]. If the desired current level is reached, the applied voltage can be reduced [6]. Various power converter topologies for the SRM drive exist in the literature. The asymmetric bridge converter is usually considered as the conventional drive [7], which utilizes two switches and two diodes per phase. This topology is used widely as it allows greater flexibility in controlling machine current and it is ideal for high-performance current and torque control, but it has high switching losses which lead the converter to require larger heat sinks. It is also not suitable for high power applications [8]. Bifilar drive structure is used in [9]. In this topology, one power switch and one diode per phase are used to regenerate the stored magnetic energy to the source. But, the use of this converter causes the need for a bifilar winding which increases the complexity of SRM. In [10], the C-dump converter is used to drive a four-phase SRM. In this topology, one switch and one diode per phase are used to charge a capacitor during the energy discharge of each phase and this topology helps to build the phase currents faster at under the base speed; however, it is not suitable for high-speed applications. Also, the dump capacitor voltage cannot be controlled since the capacitor voltage depends on the operating conditions, there is not any control over the voltage level.

The main disadvantages of the SRMs are related to the high torque ripple and acoustic noise in comparison to AC machines. In this study, a specific power converter structure is proposed as an SRM drive to reduce the torque ripple. The proposed converter has a DC-DC buck-boost converter to adjust the voltage applied to the phase windings instantaneously and a cascaded H-bridge inverter to switch the voltage polarity. The DC-DC bidirectional buck-boost converter is controlled with a sliding mode controller to have a fast and robust dynamic response. The proposed converter is able to boost the voltage to higher levels. Therefore, it can turn on and off the phases faster to minimize the commutation period, and consequently, lower torque dips occur during the commutation. Moreover, this topology helps to reduce the switching losses and eliminate the bulk DC bus capacitors. The buck feature of the converter provides a better lifetime of the machine by decreasing the current stress in the phase windings under the base speed. Furthermore, in the proposed drive system, the DC-DC conversion stage works with only one high-frequency switching per phase and H-bridge inverter only switches twice to switch the voltage polarity and apply zero voltage, which results in better converter efficiency. The proposed topology is designed as a modular structure that provides flexibility to use the system in various SRM configurations and scalability for higher power levels.

This paper is organized as follows: The proposed circuit and the control system are expressed in Section II. Section III gives a performance analysis of the driver. The conclusion of the study and future works are given in Section IV.

978-1-7281-4701-7/20/$31.00 ©2020 IEEE

II. Four-Switch Bi-Directional DC-DC Converter Topology

A. Model Description and Operating Principle

The proposed SRM drive structure is shown in Fig. 1. This structure consists of a 4-switch bi-directional DC-DC converter and an H-bridge inverter to switch voltage polarity. The DC-DC converter unit has four switches, an inductor, and an output capacitor. The inverter unit has four switches.

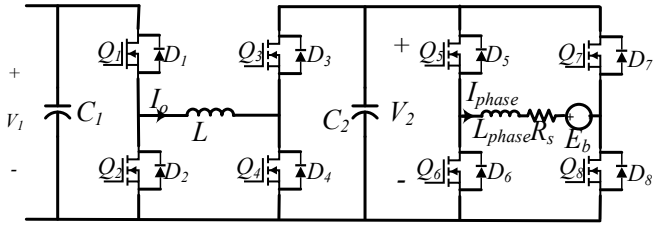

Fig. 1. Proposed SRM drive structure.

The DC-DC converter circuit is shown in Fig. 2, where V_{DC} is the input voltage, C_1 is the DC side capacitor, L and C are the inductor and the output capacitor, D_1, D_2, D_3 and D_4 are the antiparallel diodes, Q_1 , Q_2 , Q_3 and Q_4 are the switching elements, V_c and I_L are the output voltage capacitor and the inductor current.

The operating modes of the proposed DC-DC converter are given in Fig. 3. In this study, this circuit is operated in two modes: Motoring mode and Generating mode. In motoring mode, if the circuit operates as a buck converter, as given in Fig. 3(a), Q_3 is fully turned on and Q_4 is fully turned off. Q_1 and Q_2 are controlled by the PWM signal synchronously. If the circuit operates as a boost converter, as given in Fig. 3(b), Q_1 is fully turned on and Q_2 is fully turned off. Q_3 and Q_4 are controlled with alternating PWM signals.

In generating mode, if the circuit operates as a boost converter, as given in Fig. 3(c), Q_3 is fully turned on and Q_4 is fully turned off. Q_1 and Q_2 are controlled with alternating PWM signals. If the circuit operates as a buck converter, as given in Fig. 3(d), Q_1 is fully turned on and Q_2 is fully turned off. Q_3 and Q_4 are controlled with alternating PWM signals, synchronously [11].

B. Dynamic Model and State Observer of the Circuit

For the dynamic model of the circuit, the average models of buck and boost converter are considered. If the inductor current I_L and the capacitor voltage V_c are defined as x_1 and x_2, respectively, the average state equation for the buck mode is obtained as

$$\dot{x}_1 = -\frac{1}{L}x_2 + d\frac{V_{DC}}{L}$$
$$\dot{x}_2 = \frac{1}{C}x_1 - \frac{1}{RC}x_2 \quad (1)$$

Similarly, the average state equation for the boost mode can be written as

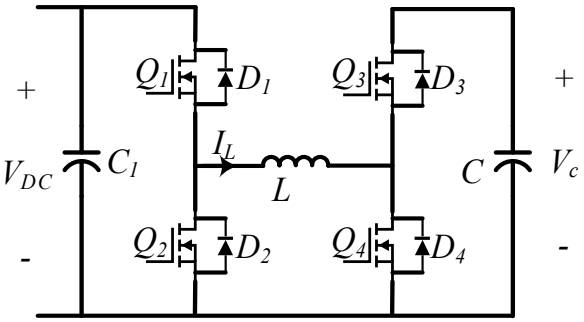

Fig. 2. 4-Switch Bi-directional DC-DC converter.

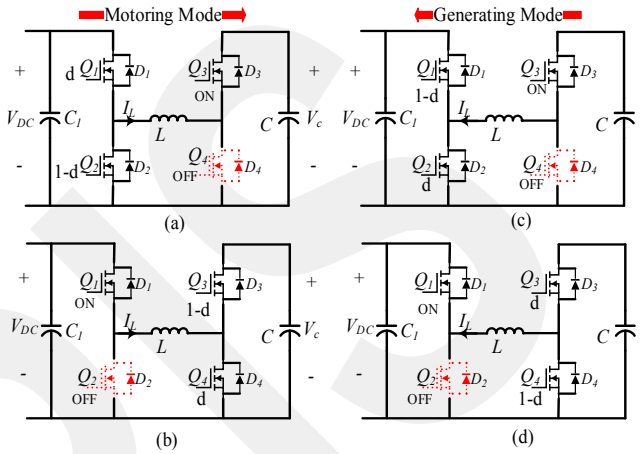

Fig. 3. (a) Buck and (b) boost in motoring mode; (c) boost and (d) buck in generating mode.

$$\dot{x}_1 = -(1-d)\frac{x_2}{L} + \frac{V_{DC}}{L}$$
$$\dot{x}_2 = (1-d)\frac{1}{C}x_1 - \frac{1}{RC}x_2 \quad (2)$$

In these equations, L is the inductor, C is the output capacitor, R is the load resistor and d is the switching signal set, $d = \{0, 1\}$. The details for the average models of the converters are given in [12].

Due to the high switching frequency of the converter, the measurement of the inductor current might be challenging. So, the inductor current should be determined without any current sensor. Hence, in this proposed converter topology, the observer is designed for estimating the inductor current. An observer equation for the buck mode is defined by

$$\dot{\hat{x}}_1 = -\frac{1}{L}\hat{x}_2 + d\frac{V_{DC}}{L} + K_1(x_1 - \hat{x}_1)$$
$$\dot{\hat{x}}_2 = \frac{1}{C}\hat{x}_1 - \frac{1}{RC}\hat{x}_2 \quad (3)$$

where $\hat{x}_1$ and $\hat{x}_2$ are the estimated variables, and K_1 is the observer gain. Let $\tilde{x}_1 = x_1 - \hat{x}_1$ and $\tilde{x}_2 = x_2 - \hat{x}_2$ be the observer errors, then using (1) and (3), the following error dynamics are obtained.

$$\dot{\tilde{x}}_1 = -\frac{1}{L}\tilde{x}_2 - K_1\tilde{x}_1$$
$$\dot{\tilde{x}}_2 = \frac{1}{C}\tilde{x}_1 - \frac{1}{RC}\tilde{x}_2 \quad (4)$$

Since the observer is constructed from the measured input and output of the system, the control input is eliminated in the error dynamics. For stability analysis of the observer, if the following candidate Lyapunov function is considered

$$V = \frac{L\tilde{x}_1^2 + C\tilde{x}_2^2}{2} > 0 \quad (5)$$

Its time derivative is

$$\dot{V} = -LK_1\tilde{x}_1^2 - \frac{1}{R}\tilde{x}_2^2 < 0 \quad (6)$$

Because the time derivative of the Lyapunov equation is negative, the observer errors converge to zero [13], [14].

Similarly, the observer equation for the boost mode from the model (2) is written as

$$\dot{\hat{x}}_1 = -(1-d)\frac{\hat{x}_2}{L} + \frac{V_{DC}}{L} + K_2(x_1 - \hat{x}_1)$$
$$\dot{\hat{x}}_2 = (1-d)\frac{1}{C}\hat{x}_1 - \frac{1}{RC}\hat{x}_2 \quad (7)$$

where $\hat{x}_1$ and $\hat{x}_2$ are the estimated variables and K_2 is the observer gain. Let the observer errors be $\tilde{x}_1 = x_1 - \hat{x}_1$ and $\tilde{x}_2 = x_2 - \hat{x}_2$, then the error dynamics for the boost observer is obtained using (2) and (7) as

$$\dot{\tilde{x}}_1 = -(1-d)\frac{\tilde{x}_2}{L} - K_2\tilde{x}_1$$
$$\dot{\tilde{x}}_2 = (1-d)\frac{1}{C}\tilde{x}_1 - \frac{1}{RC}\tilde{x}_2 \quad (8)$$

For the boost mode, if Lyapunov function (5) is used for stability analysis again, its time derivative becomes

$$\dot{V} = -LK_2\tilde{x}_1^2 - \frac{1}{R}\tilde{x}_2^2 < 0 \quad (9)$$

Again, since the time derivative of the Lyapunov equation is negative, the observer errors converge to zero for the boost mode.

C. Sliding Mode Controller

The proposed control scheme of the SRM drive is given in Fig. 4. The controller has a cascade structure with an outer linear PI voltage controller and an inner sliding mode current controller. The voltage output of the SRM is controlled with a PI controller and its output is used as a current reference to the inner sliding mode controller. The inductor current is estimated through state observers instead of physical measurements. The sliding mode controller is designed to provide robustness and fast current control response for fast reference tracking and for reducing torque ripples. The output of the sliding mode controller is the duty ratio of the PWM signal [15].

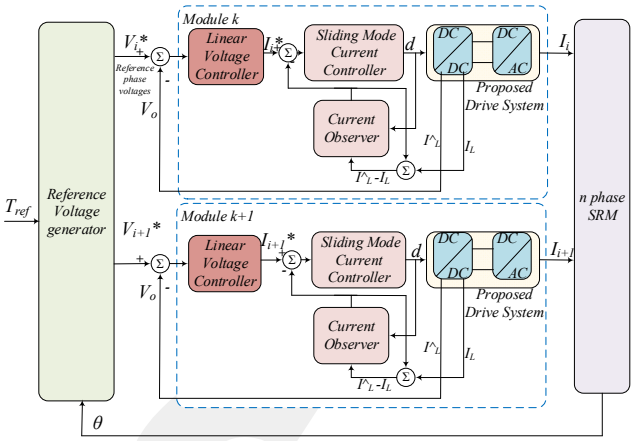

Fig. 4. The proposed control scheme of the SRM drive.

Here, the sliding surface equation for the sliding mode control is selected as

$$\hat{s} = \hat{x}_1 - x_1^* \quad (10)$$

where $\hat{s}$ is the sliding surface, x_1^* is the desired inductor current for the converter and it can be given as $x_1^* = (V_i^*)^2/RV_{DC}$, where V_i^* is the desired output voltage of the converter in i^{th} phase. With the sliding surface equation, the switching function of the converter (sliding mode controller) is defined as [15]

$$d = \frac{1}{2}(1 - \text{sign}(\hat{s})) \quad (11)$$

where the function sign$(\cdot)$ is the signum function, and the controller d takes only two values, $d = \{0,1\}$. The mode selection rule and topology for the DC-DC converter are given in Figs. 5 and 6. With the mode selection rule, the switching behaviors for the buck and boost mode of the converter are achieved. For this mode, as well as the PWM signal obtained from the SMC controller, the DC bus voltage, and the output voltage of the converter are used for the comparison [11].

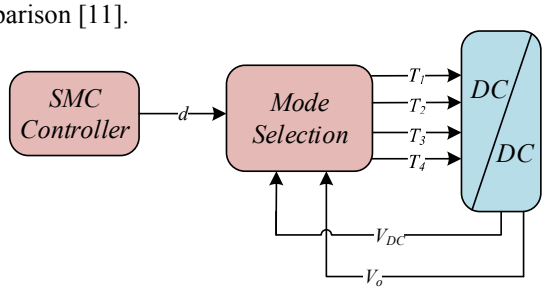

Fig. 5. The mode selection topology.

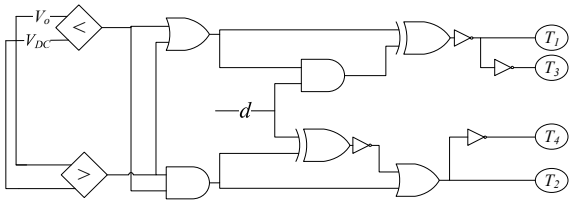

Fig. 6. The Mode selection logic.

III. Performance Analysis

The DC-DC converter for the proposed and conventional hysteresis control drive systems and the control techniques have been simulated in MATLAB/Simulink. The input voltage of the converter is selected as 200 V_{DC} and the switching frequency is selected as 150 kHz. The fixed-step solver option of ODE1 solver is used with a fixed-step of 10^{-7} seconds in Simulink to get numerical results. A 2 kW SRM is considered and with 1000 rpm base speed at 200 V DC bus voltage. The case study simulations are performed at a constant 1000 rpm.

The SRM model is built in Matlab/Simulink using the terminal voltage equations of the SRM.

$$V = R_s i + \frac{d\lambda(\theta, i)}{d\theta} \tag{12}$$

$$T(\theta, i) \tag{13}$$

where, V is the one phase terminal voltage of the SRM, R_s is the winding resistance, and λ is the flux linkage of the phase winding, T is the produced torque by that phase. The flux linkage and the torque are the functions of the rotor position and the current. Hence, the machine model requires two lookup tables to be implemented. The first one is the flux linkage versus the position and the current lookup table, and the second one is the torque versus the position and the current lookup table. These lookup tables are determined from the finite element analysis (FEA) model of the SRM.

First, the hysteresis control is simulated with the traditional converter. The optimal turn on and off angles are determined for minimum torque ripple. In this case, a minimum of 24.3% torque ripple is observed. Second, the same structure is simulated with a doubled bus voltage. Similarly, the optimal turn on and off angles are determined for minimum torque ripple. As expected, the torque ripple is reduced to 15.3% as the high bus voltage result in faster current rise and fall leading to a shorter commutation period. In this condition, one of the phase currents and the resulting voltage waveforms are captured to be used as a reference in the proposed drive system.

Later, the proposed system is simulated. A PI controller is used as the output voltage controller, and the output of a single-phase module is forced to be the captured SRM phase current waveform. The inductor current of the buck-boost converter is estimated with an observer to be used in the sliding mode controller as given in Fig. 4. The parameters used in the observer design are given in Table I.

TABLE I. Parameters Used in the Observer

Parameter	Value
R	20 Ω
L	70 μH
C	10 μF
K_1	$2000/RC$
K_2	$500/RC$

As mentioned before, the observer gains of the output voltage are selected as zero, because the output voltage is not observed for this control technique.

At 1000 rpm speed, the reference phase voltage is generated under the forced load current by the PI controller. The output voltage and current of the single-phase module of the SRM drive are given in Fig 7 and Fig. 8, respectively.

The voltage is given in Fig. 7 is rectified and used as a reference for the DC-DC converter. As seen in Fig. 4, the controller has a cascaded structure with the PI output voltage controller and sliding mode current controller. Therefore, the output of the voltage controller is used as a reference current for the inner loop sliding mode controller. This reference current is compared with the estimated inductor current via a state observer, and the sliding mode current controller is applied to have fast corrections on the required current. As mentioned earlier, the sliding mode controller uses inductor current and this current is estimated rather than measured. Calculated and observed inductor currents are presented in Fig. 9. It is clear from this figure that the sliding mode current controller tracks the reference current as desired.

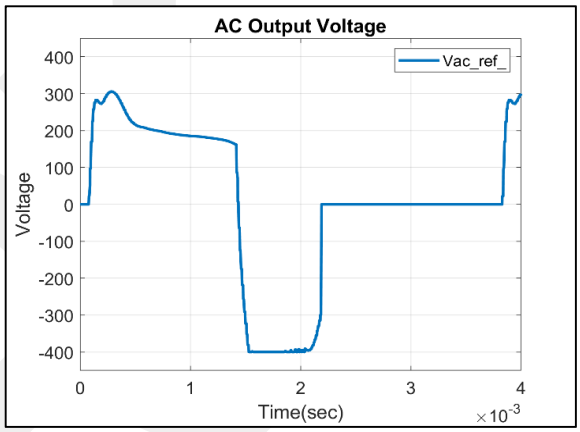

Fig. 7. The reference voltage.

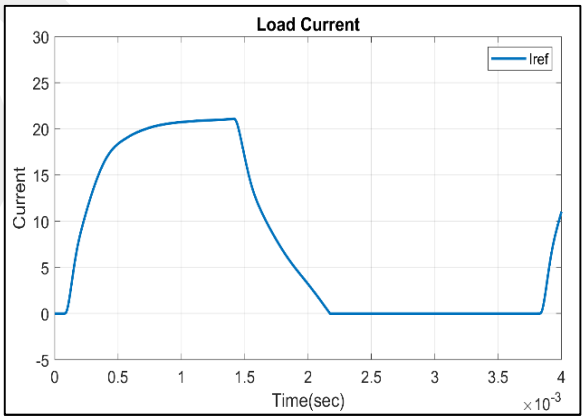

Fig. 8. The load current obtained from the SRM.

The rectified reference bus voltage and the calculated converter DC voltages are given in Fig. 10. The controller allows the output voltage to follow the reference voltage successfully.

The torque ripple minimization performance of the SRM with the proposed drive is very similar to the second hysteresis control simulation with the doubled bus voltage. The buck-boost nature of the proposed converter improved the current control during the commutation instants which resulted in shorter commutation periods and reduced torque ripple.

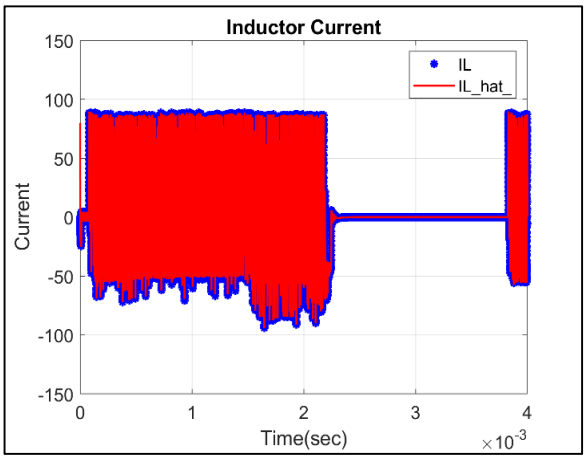

Fig. 9. The calculated and observed inductor currents.

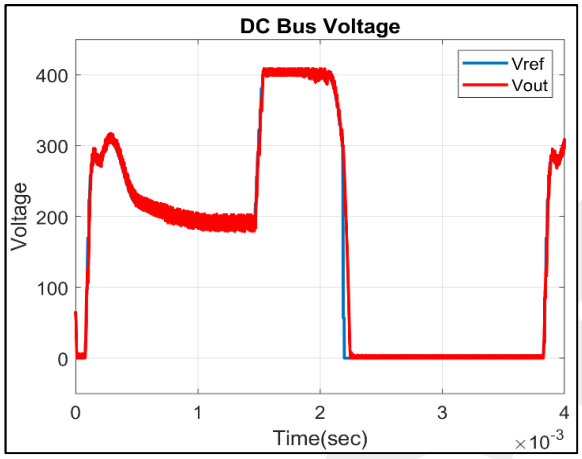

Fig. 10. The reference rectified voltage and calculated output voltage.

The calculated rectified voltage is unfolded through the H-bridge inverter. Resulting waveforms are given in Fig. 11.

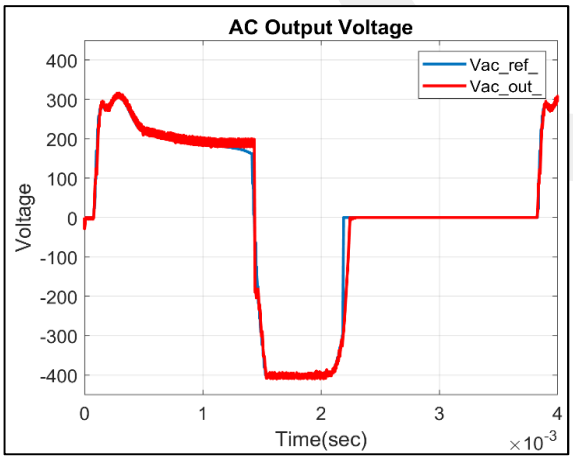

Fig. 11. The calculated output voltage in the H-bridge.

IV. Conclusion and Future Works

In this paper, a modular buck-boost SRM driver is proposed. The driver consists of a DC-DC converter and an H-bridge inverter at each phase to apply the required voltage waveforms to generate the reference currents in the motor phases. The output current is controlled with cascaded PI and sliding mode controllers. The PI controller has generated the required inductor current reference and the sliding mode controller is designed to regulate the current variations robustly with high bandwidth. The inductor current is not measured but estimated using a state observer. The desired reference waveforms are successfully generated, the conventional and the proposed drive systems are simulated to compare the performances. The simulations are performed with a 2 kW 24/16 SRM. The superiority of the proposed driver in terms of torque ripple minimization is verified by reducing the torque ripple from 24.3% to 15.3% at the base speed and rated loading condition.

The proposed drive topology provides a flexible drive system that can be configured for SRMs that has a various number of phases and powers. Hence, provides scalability for the higher power levels with multiple modular units. The buck-boost nature of the proposed driver with suitable controllers helps to control the phase currents with better precision and consequently reduces the torque ripple. This structure is well suited for applications that have limited DC voltage levels like electric bikes home appliances. Also, the proposed topology allows one to eliminate the bulky DC bus capacitors; hence, the size and the cost of the total system is reduced. Furthermore, switching losses can be reduced since most of the time only a single switch operates at high frequency, and the rest of the switches operate at low frequency.

The proposed drive topology is also suitable for improving the operation speed region when using torque sharing functions as the instantaneous voltage control feature of the proposed drive system improves the current tracking capability at high speeds.

Acknowledgment

This research is supported by The Scientific and Technological Research Council of Turkey (TUBITAK) under Grant 118E172.

References

[1] B. Bilgin, J.W. Jiang, and A Emadi, *Switched Reluctance Motor Drives: Fundamentals to Applications*. CRC Press, 2019.

[2] E. Farmahini Farahani, M. A. Jalali Kondelaji, and M. Mirsalim, "A new exterior-rotor multiple teeth switched reluctance motor with embedded permanent magnets for torque enhancement," *IEEE Transactions on Magnetics*, vol. 56, no. 2, pp. 1–5, Feb. 2020.

[3] R. Cao, E. Su, and M. Lu, "Comparative study of permanent magnet assisted linear switched reluctance motor and linear flux switching permanent magnet motor for railway transportation," *IEEE Transactions on Applied Superconductivity*, vol. 30, no. 4, pp. 1–5, Jun. 2020.

[4] E. Bostanci, M. Moallem, A. Parsapour, and B. Fahimi, "Opportunities and Challenges of Switched Reluctance Motor Drives for Electric Propulsion: A Comparative Study," *IEEE Transactions on Transportation Electrification*, vol. 3, no. 1, pp. 58–75, Mar. 2017.

[5] T. W. Lee, Y. H. Yoon, Y. C. Kim, B. K. Lee, and C. Y. Won, "Control of c-dump converters fed switched reluctance motor on an automotive application," *Electric Power Systems Research*, vol. 77, no. 7, pp. 804–812, May 2007.

[6] M. Barnes and C. Pollock, "Power electronic converters for switched reluctance drives," *IEEE Transactions on Power Electronics*, 1998.

[7] M. Ehsani, I. Husain, and A. B. Kulkarni, "Elimination of Discrete Position Sensor and Current Sensor in Switched Reluctance Motor Drives," *IEEE Transactions on Industry Applications*, vol. 28, no. 1, pp. 128–135, 1992.

[8] R. Krishnan, *Switched Reluctance Motor Drives: Modeling, Simulation, Analysis, Design, and Applications*. CRC Press, 2017.

[9] E. Afjei, M. Asgar, and S. Ataei, "A new modified bifilar drive circuit for switched reluctance motor," *in International Conference on Power System Technology and IEEE Power India Conference*, 2008.

[10] N. Inanc and V. Ozbulur, "Torque ripple minimization of a switched reluctance motor by using continuous sliding mode control technique,"

Electric Power Systems Research, vol. 66, no. 3, pp. 241–251, Sep. 2003.

[11] M. Krishnaveni, S. Rasu, "Analysis of four switch positive buck boost converter based on mode selection circuit for portable battery applications," in *IEEE Sponsored 2nd International Conference onInnovations in Information Embedded and Communication Systems ICIIECS'15*, 2015, pp. 16571–16576.

[12] V. Utkin, "Sliding mode control of DC/DC converters," *Journal of the Franklin Institute*, vol. 350, no. 8, pp. 2146–2165, Oct. 2013.

[13] S. Oucheriah and L. Guo, "PWM-based adaptive sliding-mode control for boost DC–DC converters," *IEEE Transactions on Industrial Electronics*, vol. 60, no. 8, pp. 3291–3294, Aug. 2013.

[14] H. Cho, S. J. Yoo, and S. Kwak, "State observer based sensor less control using Lyapunov's method for boost converters," *IET Power Electronics*, vol. 8, no. 1, pp. 11–19, 2015.

[15] V. I. Utkin, J. Guldner, and J. Shi, *Sliding Mode Control in Electromechanical Systems*, 2nd ed. CRC Press, 2009.